AIR MOVEMENT & VENTILATION CONTROL WITHIN BUILDINGS

12th AIVC Conference, Ottawa, Canada
24-27 September, 1991

POSTER 38

An Evaluation of a Computer Code for Predicting Indoor Airflow and Heat Transfer

Yuguo Li and Laszlo Fuchs
Dept. of Gasdynamics
Royal Institute of Technology
S–100 44 Stockholm
SWEDEN

Sture Holmberg
Ventilation Division
Institute of Occupational Health
S–171 84 Solna
SWEDEN

Synopsis

The evaluation of a code can be done by investigating two items: solving the correct equations and solving equations correctly and efficiently. An indoor airflow code VentAirI has been developed and is evaluated here. An evaluating procedure is suggested. The code is characterized by the standard high–Reynolds–number k–ε model with wall function, the two–band radiation model and the SIMPLE algorithm. Test examples are: 1. A three–dimensional forced convection problem (Re=5000), 2. A natural convection problem (Ra=$5*10^{10}$), 3. A natural convection–radiation interaction problem (Ra=$1.45*10^{9}$). All calculations are compared with experimental results and published numerical solutions. Grid refinements are used to improve the accuracy of the predictions. The applicability of the Boussinesq approximation is confirmed. The prediction of heat flux through the boundaries are, however, less accurate. The code exhibits a relatively low convergence rate; the finer the grid, the slower the convergence. A fast multi–grid solver combined with local grid refinements is suggested. Consequently, another indoor airflow code VentAirII is developed.

1. Introduction

One crucial and frequently asked question about the numerical simulation of indoor airflow is: are the accuracy and efficiency of the simulation acceptable? A good indoor airflow code should have: 1) acceptable accuracy for the predicted velocity vector, its fluctuations, the temperature fields (including radiant temperature), contaminant concentration fields and heat transfer rates through the boundaries; 2) acceptable computational cost. Not all of these features are required in all situations. The overall accuracy of the simulation can be influenced by the applicability of the turbulence model, the assumption of Boussinesq approximation, the representation of geometry, the truncation errors, and so on. The dimension of the problem and the numerical algorithm determine the computational cost. In general, confidence in the accuracy of the predictions produced by a code is obtained by investigating two items: 1) solving the correct equations, i.e. evaluating the accuracy of the physical model equations that are being used. 2) Solving these equations correctly and efficiently, i.e. evaluating the accuracy and efficiency of the numerical solution procedure for the given set of governing equations. Numerical algorithms produce only an approximate solution to the governing system of partial differential equations. Errors arise from two components of the numerical methods: discretization errors and iterative (convergence) errors .

The question of model accuracy (e.g. there exists currently no generally valid turbulence closure models) should be kept separate from the one of numerical accuracy. Thus, the various turbulence models cannot be evaluated unless the numerical accuracy is first established. The first requirement is to reduce the numerical error to an acceptable level. For any consistent numerical approximation, the error is reduced as the grid is refined. Therefore, grid refinement is a natural means of improving accuracy. In addition to grid refinement, one may also use higher order discrete approximation. However, higher order approximation can be applied only when the grid resolution is fine enough to represent the smallest length scales. Here, we shall primarily discuss the spatial resolution aspects.

For evaluating the accuracy of a numerical solution, one may resort to the following: 1). *Code to experiment comparison.* Ideally, the accuracy and limitations of the experimental data should be known and be thoroughly understood. Such kind of experimental data are rather rare, and also it should be noted that agreement with the experiment does not imply universally. A comparison between the experiment and a single shot calculation should be avoided[1]. 2). *Code to exact solution comparison.* For assessing the accuracy of a numerical method, comparison with an exact solution of the problem is the best. However, exact solutions to flow problems are known only in some simple, degenerated cases. Good accuracy in these cases does not imply similar accuracy in other general situations. 3). *Code to code comparison.* It helps to quantify numerical errors between algorithms when identical physical models are solved with different methods. But a comparison of different codes for solving the same governing equations and the same physical problem does not necessarily establish confidence, unless one of the codes has been validated for different parameter values by other means. 4) *Convergence history and spatial resolution analysis.* Slow convergence rate may mask iteration (convergence) errors. Obtaining solutions on successively finer grids reduces the truncation errors and will quantify the effect of grid resolution errors on flow quantities of interest. With Richardson extrapolation, grid refinement can be used to obtain a more accurate result, and then the accuracy of the results can be determined. Richardson extrapolation is applicable only once the asymptotic behavior of the solution is established.

The purpose of this paper is to evaluate the accuracy and efficiency of a computer code. A fast multi–grid solver combined with local grid refinements is suggested for ventilation problems. Three well–known turbulent–flow problems are selected, and computational results of the code on these problems are compared with experimental data and published numerical solutions.

2. Indoor airflow code VentAirI

2.1 Governing equations and Boundary conditions

The indoor airflow code VentAirI, which is under development by the authors, solves the unsteady, Reynolds–averaged Navier–Stokes equations along with the closure k–ε model. The equations can be written in the following conservative form:

$$\frac{\partial \varrho u_i}{\partial x_i} = 0 \tag{1}$$

$$\frac{\partial \varrho u_i}{\partial t} + \frac{\partial \varrho u_i u_j}{\partial x_j} = -\frac{\partial p}{\partial x_j} + \frac{\partial}{\partial x_j}[\mu_{eff}(\frac{\partial u_i}{\partial x_j} + \frac{\partial u_j}{\partial x_i})] - \varrho g_i \tag{2}$$

$$\frac{\partial \varrho k}{\partial t} + \frac{\partial \varrho k u_j}{\partial x_j} = \frac{\partial}{\partial x_i}[\frac{\mu_{eff}}{\sigma_k}(\frac{\partial k}{\partial x_i})] + P + G - \varrho \epsilon \tag{3}$$

$$\frac{\partial \varrho\epsilon}{\partial t}+\frac{\partial \varrho\epsilon u_j}{\partial x_j}=\frac{\partial}{\partial x_i}[\frac{\mu_{eff}}{\sigma_\epsilon}(\frac{\partial \epsilon}{\partial x_i})]+C_{1\epsilon}\frac{\epsilon}{k}(P+G)-C_{2\epsilon}\frac{\varrho\epsilon^2}{k} \tag{4}$$

$$\frac{\partial \varrho\theta}{\partial t}+\frac{\partial \varrho\theta u_j}{\partial x_j}=\frac{\partial}{\partial x_i}[\frac{\mu_{eff}}{\sigma_\theta}(\frac{\partial \theta}{\partial x_i})]+S_\theta \tag{5}$$

with,

$$\mu_{eff}=\mu+f_\mu C_\mu\varrho\frac{k^2}{\epsilon}=\mu+\mu_t \qquad P=\mu_t(\frac{\partial u_i}{\partial x_j}+\frac{\partial u_j}{\partial x_i})\frac{\partial u_i}{\partial x_j} \qquad G=\beta g_i\frac{\mu_t}{\sigma_\theta}\frac{\partial \theta}{\partial x_i} \qquad S_\theta=\frac{Q}{C_p}$$

$$C_{1\varepsilon}=1.44,\ C_{2\varepsilon}=1.92,\ \sigma_K=1.0,\ \sigma_\varepsilon=1.3,\ \sigma_\mu=0.09,\ \sigma_\theta=0.9 \tag{6}$$

where u, v *and* w are the velocity components, p is the pressure, k is the turbulent kinetic energy, ε is the dissipation rate of turbulence, μ_{eff} is the sum of the kinematic laminar viscosity μ and kinematic turbulent viscosity μ_t, C_p is the heat capacity of constant pressure, Q is the internal heat generation rate, g_i is the gravitational acceleration in direction x_i, θ is the temperature, ρ is the density (in general $\rho = \rho(\theta)$, when the Boussinesq approximation is used $\rho=\rho_{ref}$, and the buoyancy term in the momentum equation is replaced by $(\rho-\rho_{ref})g_i$, where ρ_{ref} if the reference density).

All variables are given at the supply inlets. The k and ε values are determined either by measurement or from the equations given by Awbi[2]. A zero–gradient condition applies to the exhaust outlets. At planes of symmetry, the normal gradient is zero for all quantities, and also the normal velocity components and scalar fluxes are zero. At a wall boundary, Dirichlet boundary conditions are used which are based on the wall functions for velocity, k and ε [3] and for θ [4]. For the thermal radiation, the temperature at inside surface is obtained from the energy balance equation of the surface. The radiation calculation considers both long– and short–wave radiation by a two–band radiation model[5]. The indoor air is transparent, the surfaces are grey and all energy is emitted and reflected diffusely.

2.2 Solution procedure

The equations are expressed in time–implicit and conservative finite difference form on a staggered grid. The hybrid upwind/central differencing scheme is used to discretize the advection terms. The finite difference equations are solved by the SIMPLE procedure[6]. The continuity equation is rewritten into an equation for the pressure correction. The resulting algebraic equations are solved by TDMA (Tri–Diagonal Matrix Algorithm) line–by–line method. The solutions presented here are obtained from a four to six order of magnitude reduction in the L2–norm of the residual from its maximum value. The L2–norm of the residual R is defined as:

$$R^*=[\frac{1}{6N}\sum_{i=1}^{N}(R^2_{ui}+R^2_{vi}+R^2_{wi}+R^2_{mi}+R^2_{ki}+R^2_{\epsilon i})]^{\frac{1}{2}} \tag{7}$$

The convergence rate is defined as $(R^*_{final}/R^*_{max})^{(1/N_i)}$, where N is the total number of grid points in the domain, N_i is the iteration number, R_{ui}, R_{vi}, R_{wi}, R_{mi}, R_{ki}, $R_{\varepsilon i}$ are the residuals of the three momentum equations, continuity equation and k– and ε– equations.

3. Evaluation of VentAirI

Test 1. Forced Convection

The evaluation is first carried out for a three–dimensional isothermally ventilated room for which detailed velocity field measurements are available[7]. The practical relevance of the test problem relates to mixing ventilation systems, in which air is often supplied through a small opening near the ceiling, and removed through a return opening close to the floor. The ventilated room is shown in Fig.1. The height of the room is 89 mm. Other dimensions are: is L/H=3.0; W/H=1.0; h/H=0.1; w/H=0.1. The Reynolds number, based on the inlet velocity U_{in} and the height of the inlet, is 5000. The air velocity was measured by a Laser–Doppler Anemometer. The plane y=0 is a symmetry plane. The flow is thus calculated in one half of the room only. Two grids (18*20*20 and 36*40*40) are used. The calculated profiles of longitudinal velocity u at two different z–planes (z/w=0.1 and 0.4), and corresponding measured results are given in Fig.2. The computed velocity profiles are in good agreement with the measurement. A grid–dependent solution is observed and the grid refinement improves the solution in the recirculation region.

One of the advantages of using the wall function method is that it is computationally convenient, i.e. the near–wall region is excluded from the flow domain. This does not mean that a coarse grid is adequate. It is shown here that the accuracy of the predicted velocity field can be improved by a grid refinement. The convergence rate of VentAirI is rather poor for this problem. With under–relaxation, convergence rates of only 0.986 for 18*20*20 and 0.990 for 36*40*40 can be reached. It has been observed that the convergence performance becomes even worse when the grid is finer.

Test 2. Natural Convection

The distribution of indoor air temperature is mostly non–uniform. For example, with displacement ventilation, the flow is generally driven by buoyancy forces. The buoyancy–driven flow in a cavity with differently heated vertical sides is considered here, as suggested by others[8,9]. A full–scale air–filled cavity with dimensions corresponding to the experimental results[16] is chosen here. The cavity is 2.5m high and 0.5m wide, see Fig.3. The two horizontal walls are insulated. The vertical walls are isothermal with temperatures T_h = 80°C and T_c = 34.2°C. The corresponding Rayleigh number based on the cavity height is $5*10^{10}$. The air velocities were measured by a Laser–Doppler Anemometer system. In our numerical calculation, four different uniform grids, 20*20, 40*40, 80*80 and 111*111, are used. In addition, a non–uniform grid, 53*53, is used to produce a very fine grid near the boundary and a

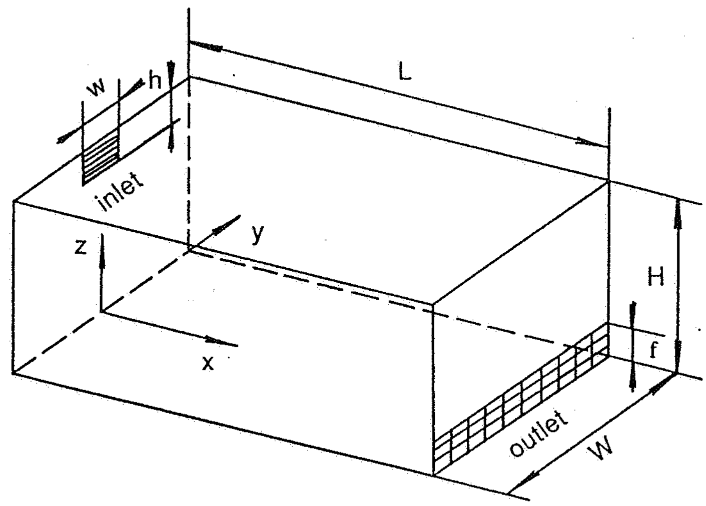

Fig.1 The experimental room for test 1.

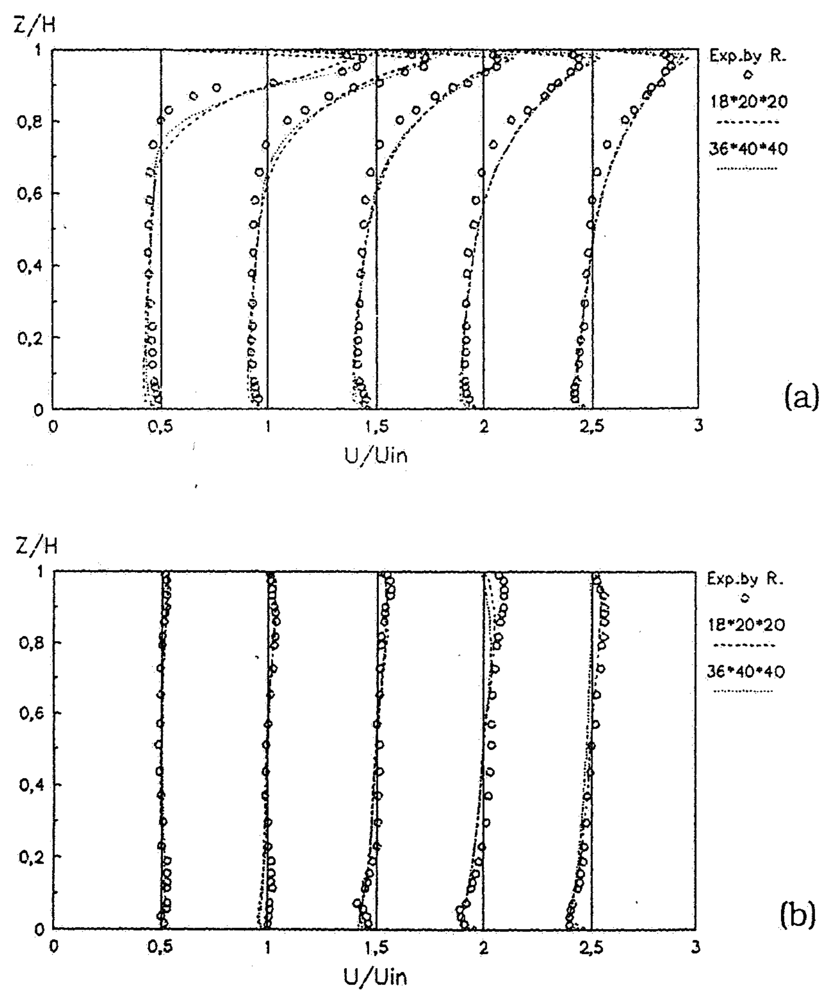

Fig.2 The calculated profiles of u–velocity component at two z–planes (a) z/w=0.1; (b) z/w=0.4.

coarse grid in the central region of the flow field. The convergence rate is in the range of 0.985–0.999.

Fig.4 compares the measured velocity profiles mid–way up the room with the ones computed by the five different grid scales. The vertical temperature profiles in the central section are given in Fig.5. Fig.6 shows the relationship between the local Rayleigh and the local Nusselt numbers. A number of observations can be made, which confirm the conclusions of Chen et al[8]: 1), a good agreement is obtained between the experiment and calculations for mid–height velocity; 2), The measured temperature of cavity in the central section is lower than the computed one. The computed one is symmetric, but not the measured. This is possibly due to the heat loss through the ceiling. There are also a number of points which emerge from a further analysis of the effects of the grid refinements. 1), Fine grid can improve the accuracy of the predicted velocity. 2), the coarse grid near the wall (20*20) gives a too–low convective heat transfer coefficient, and the fine one gives a too–high coefficient (grid 80*80 and 53*53); 3), the uniform grid 111*111 and nonuniform grid 53*53 give two almost equivalent solutions, because they use same mesh space near walls. The importance of the near wall region explains the importance of the model "wall functions" that are used.

Test 3. Natural Convection and Surface Radiation Interactions

There is more energy exchange by radiation at room temperature than is commonly realized[10], particularly when dealing with heating systems with heated surfaces and with displacement ventilation[11]. Radiation exchange between people and their surroundings is an important factor in determining thermal comfort. So the study is extended to include the interaction between natural convection and surface radiation in a square enclosure, for which the calculated results by Fugesi and Farouk[12] are used for comparison.

The geometry of the problem is shown in Fig.7. The opposing walls are maintained at two different constant temperatures, the temperature of left wall being higher than that of right wall. The floor and ceiling are thermally insulated. The surfaces of the entire enclosure are black for radiation, i.e. the wall emissivity is unity. The Prandtl number of the fluid is fixed at 0.686(CO_2). The calculation is performed for Grashof number $1.45*10^9$ and overheat ratio τ of unity (i.e. $T_h = 832.5K$, $T_c = 277.5K$). The calculations and comparison with the results of Fugesi and Farouk[12] for Grashof number $6.55*10^6$ were reported by Li and Fuchs[5]. The Boussinesq approximation is used. Gebhart's absorption method is used to calculate the radiation exchange. The present calculation is performed with a 56*56 non–uniform grid for a turbulent regime. It is impossible to get a converged solution for this problem if the number of grid points is too small and/or the grid points are not properly distributed. This is due to the bad resolution near the wall boundaries. Fig. 8 shows the temperature and flow fields with and without surface radiation. When the radiation is totally neglected, the fields are symmetric. When the surface radiation is considered, the symmetry completely disappears. The core of the fluid becomes warmer when compared to the pure natural convection case. The low–velocity region is moved from the core region to the lower part of the room, leaning toward the cold wall.

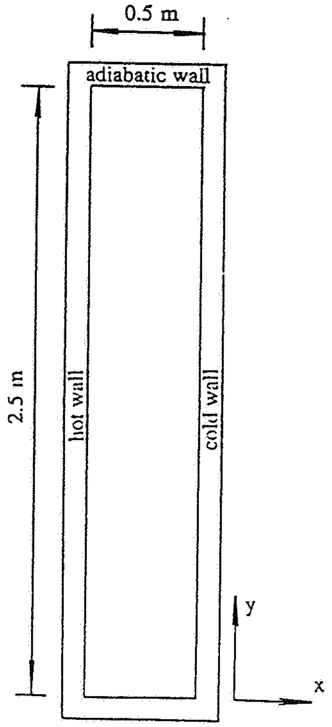

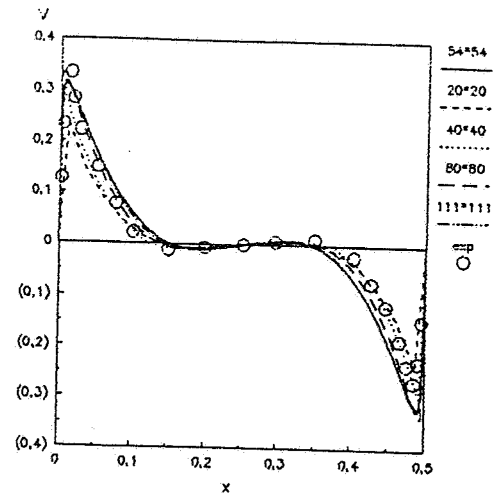

Fig.4 The measured and calculated velocity profiles mid–way up the room with five different grid spacings.

Fig.3 The full–scale air–filled cavity.

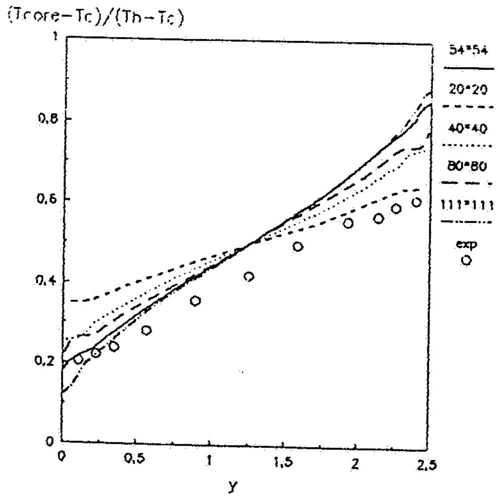

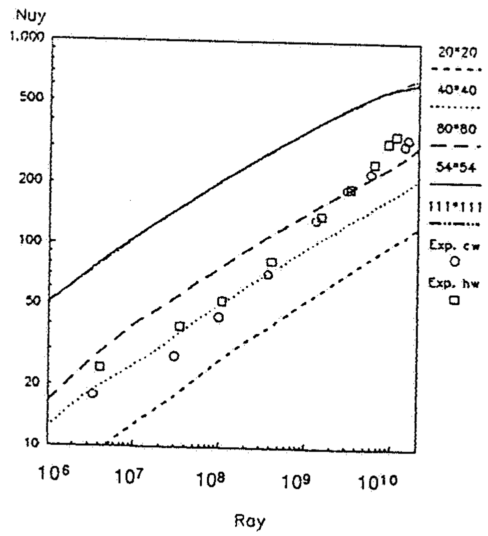

Fig.5 The measured and calculated vertical temperature profiles mid–way up the room by five different grid scales.

Fig.6 The relationship between local Rayleigh and local Nusselt numbers.

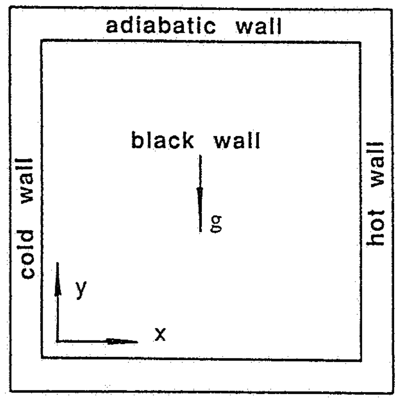

Fig.7 A square enclosure.

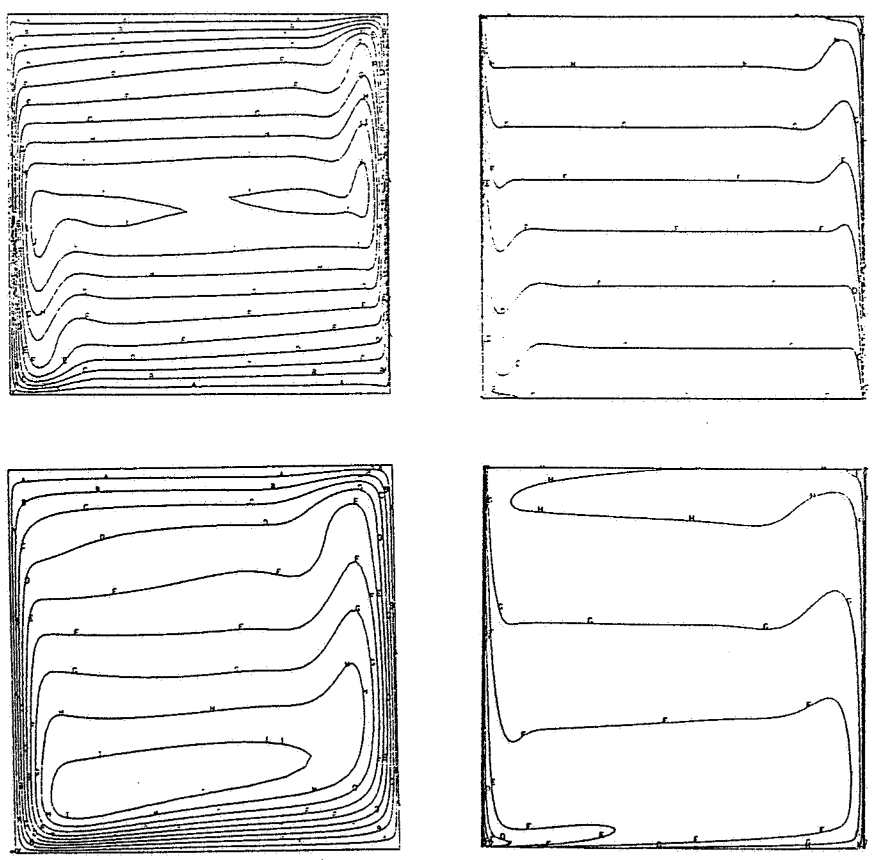

Fig.8 The flow fields (left) and temperature fields (right), with (lower) and without (upper) surface radiation.

Fig.8 is graphically identical to those of Fusegi and Farouk[12]. The velocity profiles along the midplanes of the enclosure are shown in Fig.9. The figure indicates that intense flows are induced near the insulated surfaces when radiation is taken into account. The thickness of the boundary layer in the case of turbulent regime is thinner than in the case of laminar regime[5]. The agreement between our results and the results of Fusegi and Farouk[12 is very good. The discrepancy may be due to the Boussinesq approximation in VentAirI, since the temperature difference is very large.

To further confirm the applicability of the Boussinesq approximation, the calculation is also performed without the Boussinesq approximation. The density variation due to the temperature difference is considered. The results are presented in Fig.10 for overheat ratios of 1.0 (i.e. T_h = 832.5K and T_c = 277.5K)and 0.1 (i.e. T_h = 582.75K and T_c = 527.25K). Grashof number is $6.55*10^6$.The error caused by the Boussinesq approximation is shown in the figure. When the overheat ratio is 0.1, the result considering the density variation is almost identical to the one with the Boussinesq approximation[5]. Our results with the density variation are almost identical to those of Fusegi and Farouk[12,5]. When the temperature difference is less than 50°C, the result with Boussinesq approximation is very good. So it can be concluded that for airflow simulations in ventilated rooms, the Boussinesq approximation is reasonable, since the temperature differences are very small.

4. Overview of Indoor Airflow Code VentAirII

One major numerical disadvantage of VentAirI is its slow convergence rate; the finer the grid, the slower the convergence rate. A second code VentAirII that uses the same governing equations as in VentAirI has been developed. The multi-grid (MG) procedure by Bai and Fuchs[13] and the local grid refinement procedure by Fuchs[14]and Bai and Fuchs[13] are used. The MG method is an iterative procedure which ideally exhibits a grid-independent convergence rate. The local grid refinements make it possible to resolve large gradients in the flow field without influencing the convergence rate of the MG scheme. In this new code (VentAirII), the physical domain is discretized with a global uniform rectangular mesh. In regions of high gradients, e.g. at near wall regions and at inlet/outlet regions, the locally refined mesh is added. The diffusive term is approximated by the central difference scheme. The convective term is discretized by the hybrid central/upwind differencing scheme[6]. The wall function of Launder and Spalding[15] that is used by Bai and Fuchs[13] is replaced by the wall function of Rodi[3], which means that the boundary conditions for k is changed from $dk/dn = 0$ to $k=f(u_t)$. After these modifications, it is found that the convergence performance is improved when the code is applied to the flow in an isothermal box model[13]. The Reynolds number based on the inlet width is 7000 for the isothermal flow in this box. Fig.11 shows the multigrid convergence history using a coarser grid (22*14*14*14) and a finer grid (42*26*26) with the original MG code[13] and VentAirII, respectively. The work unit is defined as the computational effort for one relaxation sweep on the finest level. The residuals are reduced 5 orders of magnitude within 35 work units with VentAirII compared 55 work units with the original MG code. The single grid results with VentAirII is also shown in the figure for comparison. The

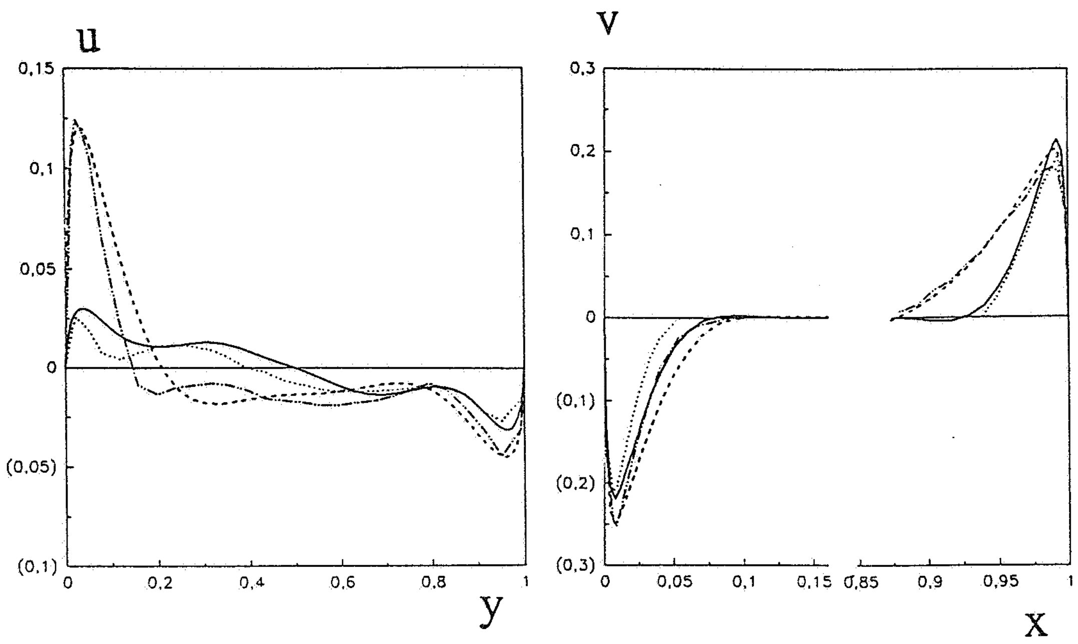

Fig.9 The velocity profiles along the mid–planes of the enclosure. ——— , no radiation; ------ , surface radiation; .... , no radiation[12]; —·—·— , surface radiation [12].

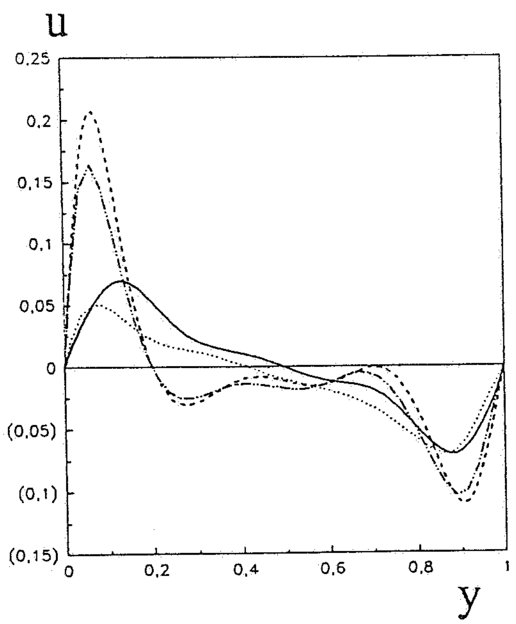

Fig.10 The velocity profiles along the mid–planes of the enclosure with (B) and without (NB) Boussinesq approximation. ——— , no radiation, τ=0.1, NB; .... , no radiation, τ=1., NB; ------ , surface radiation, τ=0.1, NB; —·—·— , surface radiation, τ=1., NB; ——— , no radiation, τ=1, B[5].

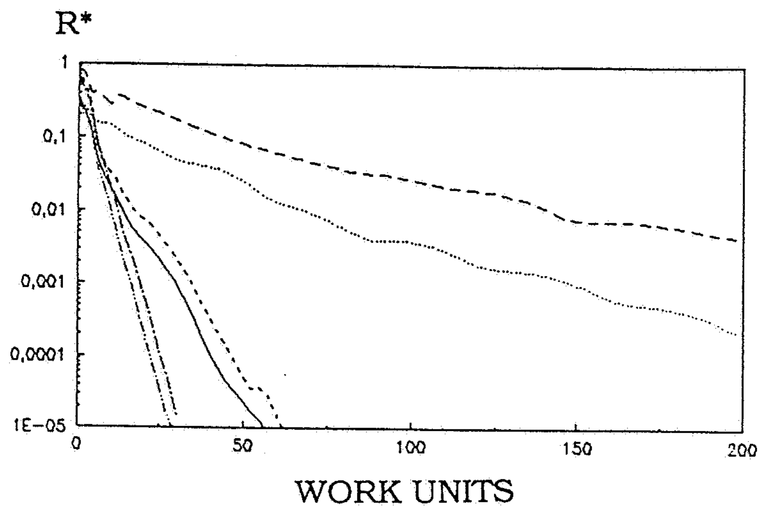

Fig.11 The convergence history of the isothermal box using single–(SG) and 3 levels multi–grid (MG) methods; results of VentAirII: —·—·— *, coarser grid, MG;* —··— *, finer grid, MG;* ·········· *, coarser grid, SG;* – – – *, finer grid, SG;* results of Bai and Fuchs[13]: —— *, coarser grid, MG;* ······ *, finer grid, MG.*

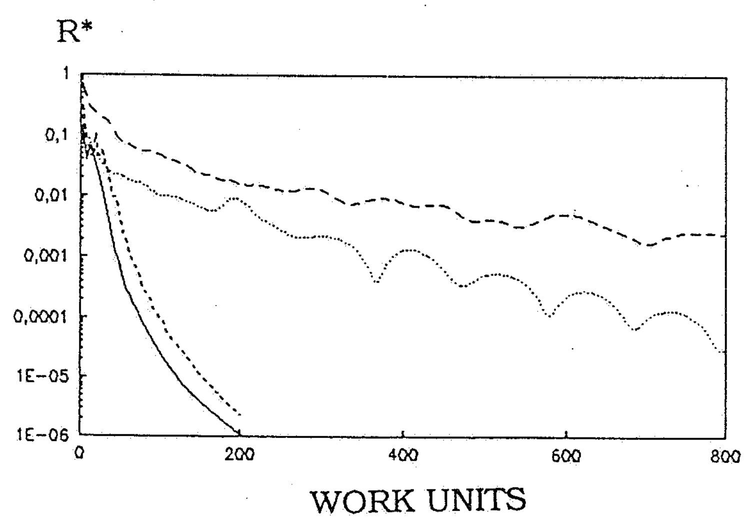

Fig.12 The convergence history of the problem in test 1 using single–(SG) and 3 levles multi–grid (MG) methods; —— *, coarser grid, MG;* ······ *, finer grid, MG;* ·········· *, coarser grid, SG;* – – – *, finer grid, SG.*

problem in test 1 is also solved by VentAirII. The VentAirI and VentAirII give identical predictions when using the same finest grid. The convergence history by VentAirII is shown in Fig.12. The coarser grid (22*14*22) and the finer grid (42*26*42) are used. The advantage of the MG method over single grid method with respect to computational speed is displayed. The computational speed with MG is a factor of 6 faster than that of the single grid for the coarser grid and a factor of 50–60 for the finer grid. The main advantage of the MG method is that the computational time is linearly increased with the number of nodes. Local refinements for the problem in test 1 can be found in Li and Fuchs[16].

5. Conclusions

Three turbulent incompressible fluid flows (forced convection, natural convection and convection–radiation interactions) have been tested to evaluate the accuracy and efficiency of the computer code VentAirI.

Solving governing equations correctly and efficiently. The grid refinement studies here indicate that grid fineness can improve the accuracy of the predicted velocity and temperature fields. Grid refinement is also expected to reduce the numerical diffusion. Fine grids and a proper distribution of the grid points are required to get an accurate numerical solution. The usage of a large number of computational elements requires faster convergence. The convergence test shows that VentAirI exhibits a low convergence rate; and the finer the grid the slower the convergence. The problem can be overcome by the MG method together with local grid refinements. This has been demonstrated by VentAirII. A nearly grid–independent convergence has been achieved for the test problems with more than an factor 50 reduction in CPU time for the finer grid. Thus the fast MG solver combined with local grid refinements is very appropriate for ventilation problems

Solving correct governing equations: The applicability of the Boussinesq approximation is confirmed. The results from the various grid scales differ most for quantities that are determined in the inner layer of the boundary layer, for example, the wall heat transfer. This implies that the high–Reynolds–number model with wall functions is not suitable for simulating indoor air flow from the heating and cooling load point of view. HAVC engineers are interested in heat loss and heat gain through the boundaries. Possible improvements to the turbulent model may include improving the wall function treatment or rather eliminating the need for a too coarse scale modelling (using Large Eddy Simulation). Experiments should also be designed properly, so that the produced data are relevant and accurate for code validation.

6. Acknowledgement

This work was financially supported by the Swedish Council for Building Research (BFR). We would like to thank deeply Dr. X.S. Bai for his help in adapting the 3D MG code into VentAirII.

7. References

1. ROACHE, P. J. "Need for control of numerical accuracy", Journal of Spacecraft and Rockets, vol. 27, no. 2, pp. 98–102, 1990.

2. AWBI, H. B. "Application of computational fluid dynamics in room ventilation", Building and Environment, vol.24 no.1, pp.73–84, 1989.

3. RODI, W. "Turbulence models and their application in hydraulics", International Association of Hydraulic Research, Monograph, Delft, 1980.

4. JAYATILLIAKA, C. L. V. Progr. in Heat Mass Transfer, vol.1 pp. 193, 1969.

5. LI, Y., FUCHS, L. "A two–band radiation model for calculating room wall temperature", 1st Baltic Heat Transfer Conference, Göteborg, Sweden, 26th–31st, August, 1991.

6. PATANKAR, S. K. "Numerical Heat Transfer and Fluid Flow", Hemisphere Publishing Corp., Washington, D.C., 1980.

7. RESTIVO, A. "Turbulent flows in ventilated rooms". PhD thesis, Dept. of Mech. Eng., Imperial College, London, 1979.

8. CHEN, Q.Y., MOSER, A., HUBER, A. "Prediction of buoyant, turbulent flow by a low Reynolds number k–e model", ASHRAE Transactions, 1990.

9. BAKER, A. J., KELSO, R.M. "On validation of computational fluid dynamics procedure for room air motion prediction. ASHRAE Transactions, vol.96, part1, 1990.

10. MCINTYRE, D. A. "The thermal radiation field", Building Science, vol.9, pp.247–262, 1974.

11. HEISEILBERG, P., SANDBERG, M. "Convection from a slender cylinder in a ventilated room", Proceedings of Roomvent'90, Oslo, Norway, June 13–15, 1990.

12. FUGESI, T., FAROUK, B. "Laminar and turbulent convection–radiation interactions in a square enclosure filled with a monger gas", Numerical Heat Transfer, part A, vol.15, pp.303–322, 1989.

13. BAI, X. S., FUCHS, L. "A fast multi–grid method for 3–D turbulent incompressible flows", 7th International Conference on Numerical Methods in Laminar and Turbulent Flow, Stanford, California, 15th–19th July, 1991.

14. FUCHS, L. "A local mesh–refinement technique for incompressible flows", Computers & Fluids, vol. 14, no.1, pp.69–81, 1986.

15. LAUNDER, B.E., SPALDING, D.B. "The numerical computation of turbulent flows", Comp. Math. in Appl. Mech. & Engi. 3, pp.269–289, 1974.

16. LI, Y., FUCHS, L., BAI, X.S."Accurate numerical simulation of air flows in ventilated multi–rooms", Building Simulation'91, Nice, Sophia–Antipolis, France, 20th–22nd, August, 1991.

17. CHEESEWRIGHT, R., KING, K.J., ZIAI, S. "Experimental data for the validation of computer codes for the prediction of two–dimensional buoyant cavity flows", Significant Questions in Buoyancy Affected Enclosure or Cavity Flows. ed. Humphrey, J.A.C. et al, pp.75–81, New York, ASME, 1986.